

Alma Mater Studiorum Università di Bologna  
Archivio istituzionale della ricerca

Green Fabrication of (6,5)Carbon Nanotube/Protein Transistor Endowed with Specific Recognition

This is the final peer-reviewed author's accepted manuscript (postprint) of the following publication:

*Published Version:*

Green Fabrication of (6,5)Carbon Nanotube/Protein Transistor Endowed with Specific Recognition / Berto M.; Di Giosia M.; Giordani M.; Sensi M.; Valle F.; Alessandrini A.; Menozzi C.; Cantelli A.; Gazzadi G.C.; Zerbetto F.; Calvaresi M.; Biscarini F.; Bortolotti C.A.. - In: ADVANCED ELECTRONIC MATERIALS. - ISSN 2199-160X. - ELETTRONICO. - 7:5(2021), pp. 2001114-2001114-2001114. [10.1002/aelm.202001114]

*Availability:*

This version is available at: <https://hdl.handle.net/11585/849526> since: 2022-01-31

*Published:*

DOI: <http://doi.org/10.1002/aelm.202001114>

*Terms of use:*

Some rights reserved. The terms and conditions for the reuse of this version of the manuscript are specified in the publishing policy. For all terms of use and more information see the publisher's website.

This item was downloaded from IRIS Università di Bologna (<https://cris.unibo.it/>).  
When citing, please refer to the published version.

(Article begins on next page)

## **Green fabrication of (6,5)CNT/protein transistor endowed with specific recognition**

*Marcello Berto, Matteo Di Giosia, Martina Giordani, Matteo Sensi, Francesco Valle, Andrea Alessandrini, Claudia Menozzi, Andrea Cantelli, G. Carlo Gazzadi, Francesco Zerbetto, Matteo Calvaresi\*, Fabio Biscarini and Carlo A. Bortolotti\**

Dr. M. Berto, Dr. M. Giordani, Dr. M. Sensi, Prof. F. Biscarini, Dr. C.A. Bortolotti  
Dipartimento di Scienze della Vita - Università di Modena e Reggio Emilia, Via Campi 103,  
Modena 41125, Italy  
Email: [carloaugusto.bortolotti@unimore.it](mailto:carloaugusto.bortolotti@unimore.it)

Dr. Matteo Di Giosia, Dr. A. Cantelli, Prof. Francesco Zerbetto, Prof. Matteo Calvaresi  
Dipartimento di Chimica “Giacomo Ciamician”, Alma Mater Studiorum - Università di Bologna,  
Via Francesco Selmi 2, 40126 Bologna, Italy  
Email: [matteo.calvaresi3@unibo.it](mailto:matteo.calvaresi3@unibo.it)

Dr. F. Valle  
CNR - Istituto per lo Studio di Materiali Nanostrutturati, Via P. Gobetti, 101, 40129, Bologna,  
Italy

Dr. F. Valle  
Consorzio Interuniversitario per lo Sviluppo dei Sistemi a Grande Interfase (CSGI), via della  
Lastruccia 3, 50019 Firenze, Italy

Prof. A. Alessandrini, Dr. C. Menozzi, Dr. G.C. Gazzadi  
CNR - Istituto Nanoscienze, S3, Via Campi 213/A, 41125, Modena, Italy

Prof. A. Alessandrini, Dr. C. Menozzi  
Dipartimento di Scienze Fisiche, Informatiche e Matematiche, Università di Modena e Reggio  
Emilia, Via Campi 213/A, 41125, Modena, Italy

Prof. F. Biscarini  
Center for Translational Neurophysiology - Istituto Italiano di Tecnologia  
Via Fossato di Mortara 17-19, Ferrara 44100, Italy

Keywords: carbon nanotubes, lysozyme, EGT, biosensor, green chemistry

## ABSTRACT

A general single-step approach is introduced for the green fabrication of hybrid biosensors from water dispersions. The resulting device integrates the semiconducting properties of a CNT and the functionality of a protein. In the initial aqueous phase, the protein (viz., lysozyme) disperses the (6,5) CNT. Drop casting of the dispersion on a test pattern, with interdigitated Au source and drain electrodes on silicon wafer, yields a fully operating robust electrolyte-gated transistor (EGT) in one step. The EGT response to biorecognition is then assessed using the lysozyme inhibitor N-acetyl glucosamine trisaccharide. Analysis of the output signal allows us to extract a protein-substrate binding constant in line with values reported for the free (without CNT) system. The methodology is robust, easy to optimize and re-direct towards different targets, and sets the grounds for a new class of CNT-protein biosensors that overcome many limitations of the technology of fabrication of CNT biosensors.

## 1. Introduction

Bioelectronics links bio-based signals and electronics by means of transducers units. Commercially available examples of bioelectronic devices include blood glucose sensors, deep-brain stimulators, neural prosthetics, and cardiac pacemakers.<sup>[1–4]</sup> The decrease of the size and physical dimension of the transducers will attenuate their invasiveness, yielding a reduced reaction of the living organism against a foreign object along with the enhancement of the signal-to-noise ratio and higher spatio-temporal resolution. The ultimate move from bioelectronics to nano-bioelectronics<sup>[5,6]</sup> will exploit nanowires, low dimensional materials, and nanostructured carbon allotropes such as Carbon Nanotubes (CNT). These promising candidates for high performing transducers are characterized by outstanding electronic properties.<sup>[7–16]</sup> In particular, the interest for CNTs as biosensor components<sup>[17–25]</sup> is further supported by their exceptional electrical performances, even at small applied potential ( $< 1\text{V}$ ). CNT-field-effect transistor-based biosensors have shown great potential for ultrasensitive biomarker detection, but challenges remain, which include difficulty in stable functionalization, incompatibility with scalable fabrication, and nonuniform performance.<sup>[26]</sup>

Insolubility both in water and organic solvents and high tendency to aggregate hinder their wide applicability, therefore methods enabling their processability are needed.

Carbon nanotubes are dispersed either mechanically or chemically. The direct “mechanical” methods tend to have low efficiency and to yield poor stability of the dispersion. The “chemical” covalent approach functionalizes the CNT walls with chemical moieties. It improves solubility in solvents and reduces the tendency to agglomerate,<sup>[27]</sup> but it remains an aggressive methodology prone to cause defects on the CNT walls that can ultimately modify their peculiar electrical

properties, which are crucial for their applications in FET. Of these approaches, the noncovalent functionalization is particularly attractive since it preserves the characteristic electronic properties of the CNT and can exploit a variety of molecules, surfactants, polymers and biomolecules.<sup>[28–32]</sup>

The technological shift from transducers to biosensors requires the integration of a specific recognition unit in the electronic transducer that, in the case of CNT-based biosensors, may follow different alternatives such as covalent attachment (tethering),<sup>[33]</sup> non-covalent adsorption using linker molecules,<sup>[34,35]</sup> direct adsorption via hydrophobic or electrostatic interactions with the tube surface<sup>[31,36,37]</sup> or entrapment in a polymeric matrix.<sup>[38]</sup>

In this work, we use a protein, namely lysozyme, as dispersant agent for a selected CNT, the semiconducting single wall (6,5)CNT.<sup>[39]</sup> The use of lysozyme (LZ) enables processability of the (6,5)CNT on one hand, on the other hand it introduces the protein directly on the semiconducting surface.<sup>[40]</sup> The wild type protein can be used directly without the modification that a tethering approach would require. This approach produces a highly stable hybrid characterized by a large interaction energy between CNT and protein.<sup>[41]</sup> Yet, it retains the electronic properties of the CNT and the full protein functionality.<sup>[42]</sup> The procedure proposed here (a) affords green water-processing of the system to produce an Electrolyte-Gated Transistor (EGT), and (b) endows the (6,5)CNT-based active channel with the additional functionality of biorecognition. The LZ/(6,5)CNT hybrid works both as a semiconductor layer and as a recognition element. The device is fabricated by a one-step self-organized process and overcomes several severe limitations that exist in the present technology for the fabrication of robust CNT transistors: the proposed strategy allows to deposit the semiconductive channel in a fast, easy way and from aqueous

solution, while most of the CNT-based transistor described in previous works require organic solvents,<sup>[43,44]</sup> the application of external electrical potential to orientate the carbon nanotubes during the deposition<sup>[43,44]</sup> or of specific fabrication techniques such as chemical vapor deposition or spray-coating.<sup>[45,46]</sup>

## 2. Results and discussion

LZ/(6,5)CNT hybrids were synthesized by ultrasonication of (6,5)CNT powder in an aqueous solution of lysozyme.<sup>[47,48]</sup> The solution was centrifuged and the supernatant was collected. The UV-vis spectrum of LZ/(6,5)CNT showed a band centered at 280 nm, typical of the protein, and the E11 and E22 transitions of the (6,5)CNTs (**Figure S1a**). (6,5)CNTs are dominant in the sample. Atomic force microscopy (AFM) images (**Figure S2a**) of the deposited LZ/(6,5)CNT hybrids is a clear evidence of the presence of highly dispersed and debundled LZ/(6,5)CNT adducts in the aqueous systems.

Electrolyte-gated transistors were first fabricated by drop casting of a 150  $\mu\text{g/ml}$  aqueous solution of LZ/(6,5)CNT hybrids on a silicon substrate to bridge interdigitated Au source and drain electrodes (width/length, W/L, equal to 560) on a test pattern (**Figure 1a**). The channel formed by the randomly oriented LZ/(6,5)CNT hybrids network is gated by a Pt wire immersed in 50 mM PBS.

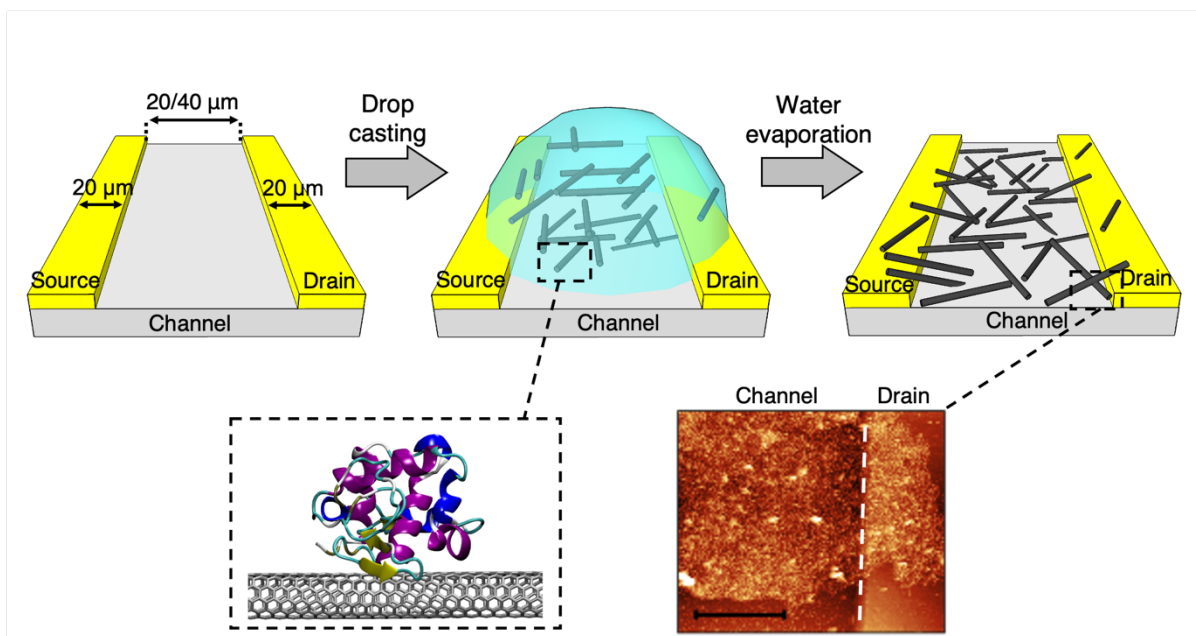
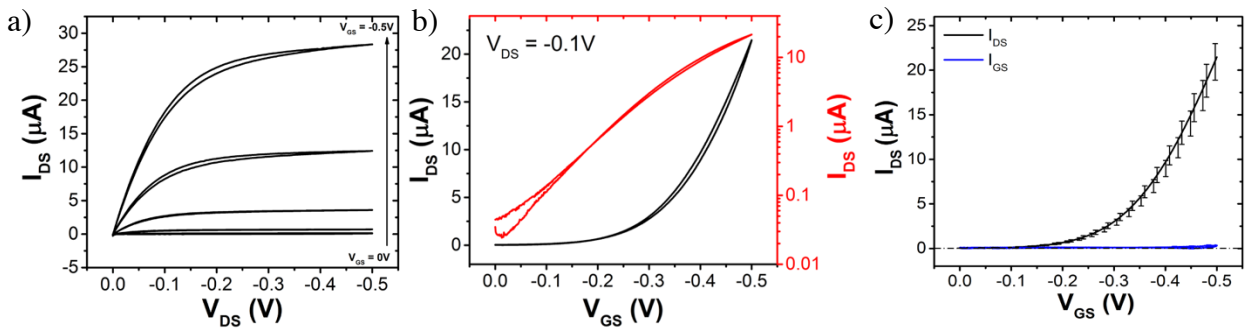


**Figure 1.** Fabrication procedure of LZ/(6,5)CNT-based EGTs: (top) from left to right, deposition by drop casting of the LZ/(6,5)CNT water dispersion on a clean silicon wafer surface by drop casting; after water evaporation, few nanotubes bundled are present on the surface (average CNT length = 1  $\mu\text{m}$ ); (bottom) in the bottom left panel, one of the potential interaction geometries between a lysozyme molecule and a (6,5)CNT is schematically depicted, and in the bottom right panel, AFM image of LZ/(6,5)CNT bundles (the bar corresponds to 5  $\mu\text{m}$ ) is shown.

**Figure 2a** and **Figure 2b** show the typical output and transfer characteristics (the former  $I_{\text{DS}}$  vs.  $V_{\text{DS}}$ , at constant  $V_{\text{GS}}$  values in the 0 V  $\div$  -0.5 V range; the latter  $I_{\text{DS}}$  vs.  $V_{\text{GS}}$ , at constant  $V_{\text{DS}}$  = -0.1 V) of a p-type semiconductor, with the drain current increasing as  $V_{\text{GS}}$  becomes more negative. Importantly, (6,5)CNTs from the same batch dispersed with the surfactant SDS (sodium dodecyl sulphate) and drop-cast on same test patterns do not exhibit current modulation in the same gate voltage range (**Figure S3**). Atomic Force Microscopy characterization of the SDS/

(6,5)CNTs dispersion revealed that it is mainly characterized by bundles and ropes (Figure S2b). The bundling of the semiconducting (6,5)CNT to ropes is known to result in a decrease of the energy gap<sup>[49]</sup> and a metallicity character appears, as confirmed here by electrical measurements on SDS/(6,5)CNTs EGOT. The control experiment with SDS/(6,5)CNTs suggests that LZ is a more effective dispersant agent for (6,5)CNT than SDS, and that the use of LZ as dispersant fully preserves the semiconducting character of (6,5)CNTs. While SDS molecules non-specifically adsorb on the tube surface, and bundling and roping phenomena appear, the specific interaction between proteins and carbon nanotubes, based on shape complementarity, disperses the carbon nanotube monomolecularly, preserving the electronic properties of the tubes.<sup>[37,41]</sup>

We ascribe the observed electrical response of the LZ/CNT EGT to the field effect caused by ions migration forming electrical double layers at the gate/electrolyte and electrolyte/LZ/CNT



interfaces. The current modulation arises from a change of the electronic charge density within the semiconducting material. The saturation current in Figure 2a is reached at relatively low drain voltages (around -0.25 V). The LZ/(6,5)CNT EGTs exhibit optimal operation, as witnessed by the almost negligible hysteresis (Figure 2b) and by the average threshold voltage,  $V_{th} = -331$  ( $\pm 10$ ) mV, the latter value ensuring operation at low biasing voltages. To assess the robustness of the device response, eight different LZ/(6,5)CNT EGTs were fabricated and their transfer



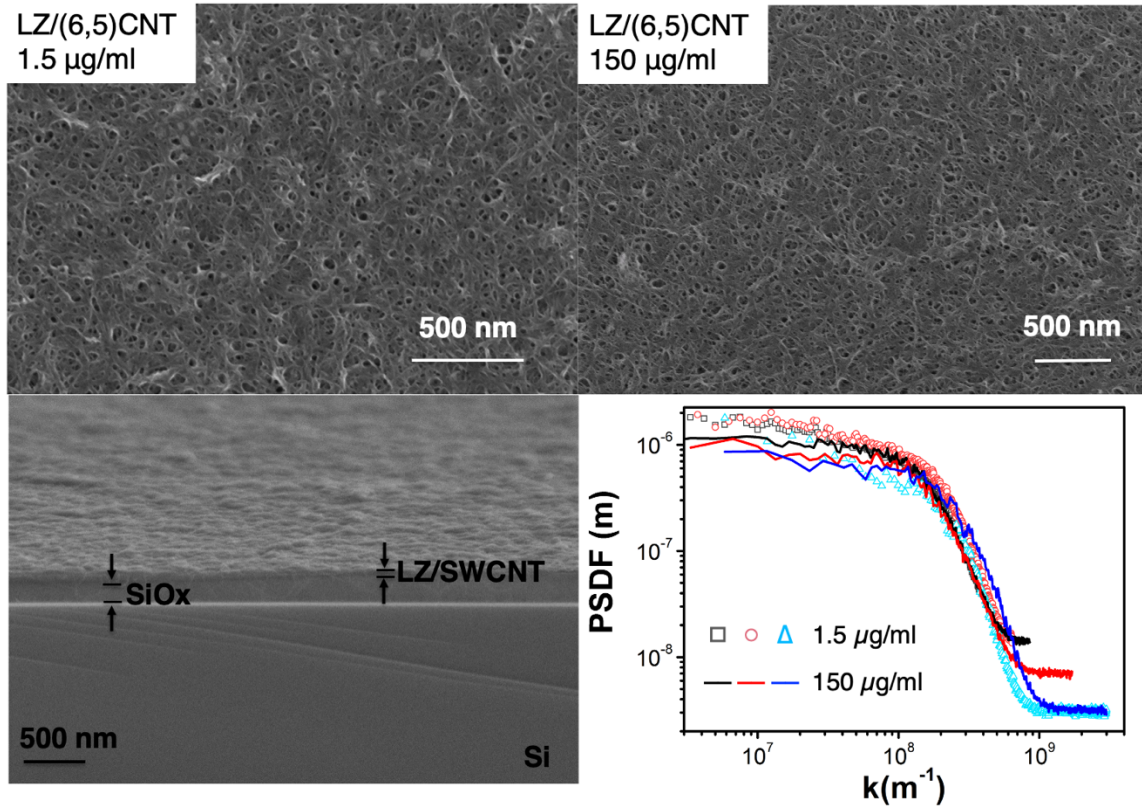
characteristics were measured. Figure 2c shows their average transfer curve: the fabrication procedure shows remarkably high reproducibility, which is one of the advantages of the use of networks made by a selected CNT over single tube devices, the latter prone to sizable fluctuations due to the individual nature of the channel.<sup>[18]</sup> These findings indicate that the protein dispersion is able to overcome two recurrent issues, i.e. i) high tendency of the CNT to aggregate, forming bundles and ropes that degrade their semiconducting characteristics, and ii) the scarce stability of CNTs in transistors, affecting the electrical response of solution-processed (6,5)CNTs.<sup>[50]</sup>

**Figure 2.** LZ/(6,5)CNT EGOT (a) output characteristics recorded for  $I_{GS} = 0 \text{ V} \div -0.5 \text{ V}$ ; (b) lin-lin (black) and semilog (red) transfer characteristics; (c) average transfers characteristics recorded at  $V_{DS} = -0.1 \text{ V}$ ; in black the channel current  $I_{DS}$ , in blue the leakage current  $I_{GS}$ . Error bars correspond to the rms of the current averaged over eight devices.

The average transconductance  $g_m = 137 (\pm 4) \mu\text{S}$  and the on/off ratio of about 778. The moderate on/off ratio can be ascribed to high off current values as shown in Figure 2b, which can result either from the presence of a residual small population of metallic tubes in the channel or from sizable leakage currents arising from the exposure of the source electrode to the electrolyte (see Figure 1c). The latter factor, due to low CNT coverage on electrodes, would be however endemic to all CNTs transistors.<sup>[11,17]</sup> We assessed the possibility of depositing a semiconducting LZ/(6,5)CNT channel from a more diluted solution: we could obtain a working transistor using a LZ/(6,5)CNT concentration as low as  $1.5 \mu\text{g/ml}$ , while lower concentrations did not yield a semiconducting channel, most likely due to the fact that continuous pathways bridging source

and drain were not connected as a consequence of the low density, thus being apparently below the percolation threshold.<sup>[51]</sup> The electrical performances of the CNT EGTs fabricated by drop casting of a 1.5  $\mu\text{g/ml}$  solution are in line with other reported semiconducting (6,5)CNT field-effect transistors,<sup>[17,50]</sup> though worse than those obtained from the 100-times more concentrated hybrid CNT/protein solution, as reported in **Table S1** and **Figure S4** and **Figure S6**. In order to test the possibility of translating our fabrication procedure to a different, widely used, substrate, we deposited 1.50  $\mu\text{g/ml}$  LZ/(6,5)CNT solution on quartz, instead of the Si wafer, with Au source and drain interdigitated electrodes (see **Figure S5**). The performances of Si-based and quartz-based devices are comparable, as reported in Table S1. We rationalize the differences of the electrical performances between the devices prepared from 1.5  $\mu\text{g/ml}$  solution and 150  $\mu\text{g/ml}$  solution in terms of morphology of the semiconductive film. In our devices, charge transport (hence output current, on/off ratio and transconductance) relies on the LZ/(6,5)CNT percolation network connecting source and drain electrodes. Atomic force microscopy (AFM) (Figure 1) shows that the channel consists of a dense network of LZ/(6,5)CNT, that nevertheless covers only a limited area of the channel. Source and drain electrodes are partially covered by LZ/(6,5)CNT, while most of their area is left completely bare, thus in direct contact with the electrolyte. This is observed at both concentrations. This situation will affect charge injection as well as the effective W/L ratio of the transistor characteristics. We infer that both concentrations are well above percolation threshold, the most influential factor will be the effective width. This is confirmed by the morphology of LZ/(6,5)CNT percolation networks measured by Scanning Electron Microscopy (SEM) as shown in **Figure 3**. The SEM images and their Power Spectral Density Function (PSDF) analysis show that, despite the different initial concentration of **LZLys/**

(6,5)CNT solution, the resulting bundles are characterized by a similar porous morphology. The PSDF spectra for both concentrations are very similar, in particular the bending of the initial



plateau towards a linear self-affine dependence takes place at the same values of  $k$ , corresponding to a characteristic length of about 40 nm, that can be associated to the average pore diameter observed in Figure 3a and 3b. Despite the fact that topography is indirectly embedded in the intensity of the signal, which makes the consideration by and large qualitative, the PSDs hint to a greater roughness, and hence thickness, of the deposit from the more concentrated solution. This is confirmed by the measurement of thickness of LZ/(6,5)CNT bundles (Figure 3c) from cross-section SEM: bundles formed from the more concentrated solution are thicker ( $141 \pm 57$  nm), conversely the ones from the less concentrated solution are thinner and more homogeneous ( $42 \pm 19$  nm). The scaling of the transconductance (see Table S1)

c)

d)

mirrors the thickness increase of the film with the concentration. This bears similarity with the observed behavior of conductive polymers, such as PEDOT:PSS in organic electrochemical transistors, whose porous morphology is associated to the so-called volumetric capacitance.<sup>[52,53]</sup>

As can be observed from the transfer curves (semilog format) in Figure 2b, the higher on/off ratio is mostly caused by the lowering of the off-current (more than five times smaller) with respect to the enhancement of the maximum current (about two times).

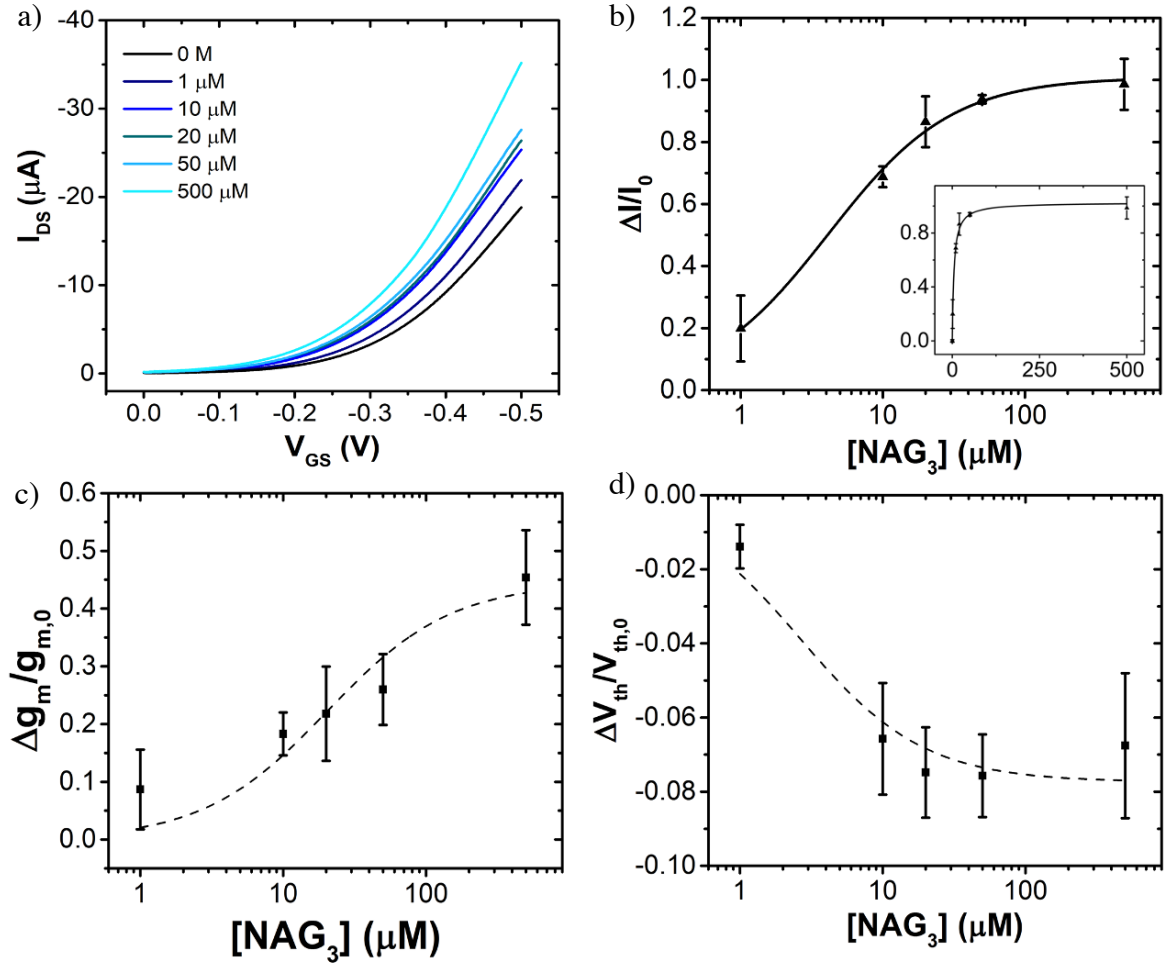
**Figure 3.** SEM images of LZ/(6,5)CNT networks on Si substrate formed from (a) 1.5  $\mu\text{g/ml}$  solution; (b) 150  $\mu\text{g/ml}$  solution; (c) SEM cross-section of LZ/(6,5)CNT layer on Si test pattern; the Si substrate, the SiO<sub>x</sub> dielectric layer and the semiconductive film are visible; (d) PSDF of the images of the LZ/(6,5)CNT networks for 1.5  $\mu\text{g/ml}$  (open symbols) and 150  $\mu\text{g/ml}$  (lines).

Up to this point, we have demonstrated that LZ is an effective dispersive agent for (6,5)CNT, that enables the processing of (6,5)CNT in aqueous environment. Moreover, the non-covalent lysozyme-(6,5)CNT interaction preserves the semiconducting behavior of the (6,5)CNTs.

For biosensing purposes, it is important to assess that the dispersing protein maintains its functionality. It is well-known that upon interaction with CNTs, lysozyme preserves its activity.

[54–56]

**Figure 4.** (a) Transfers characteristics upon exposure to different concentrations of NAG<sub>3</sub> ( $V_{\text{DS}} = -0.1 \text{ V}$ ). NAG<sub>3</sub> concentrations are reported in the inset; (b) biosensor dose curve  $\Delta I/I_0$  vs [NAG<sub>3</sub>] calculated at gate-source potential  $V_{\text{GS}} = -0.3 \text{ V}$ . In the inset the dose curves in lin/lin scale; (c) relative variation of transconductance ( $g_{\text{m}}$ ) and (d) threshold voltage ( $V_{\text{th}}$ ) vs NAG<sub>3</sub>



concentration. Error bars correspond to the signal averaged over five devices. The data in panel (b), (c) and (d) are fitted with Langmuir equation (equation 1).

To assess the conservation of lysozyme recognition ability, we used the electrolyte-gated (6,5)CNT transistor as a biosensor to record variations of the electrical response in the presence of increasing concentrations of N-acetyl glucosamine trisaccharide (NAG<sub>3</sub>), which is a well-known substrate analogue/inhibitor for this enzyme.<sup>[57]</sup> The results are reported in **Figure 4**. Transfer characteristics (Figure 4a) change monotonically with the increasing concentration of

NAG<sub>3</sub> (from 1  $\mu\text{M}$  to 500  $\mu\text{M}$ ); in particular the output current  $I_{\text{DS}}$  increases when NAG<sub>3</sub> is detected by the transistor.

To minimize device-to-device variability, we build the dose curve that represents the relative average variation of  $I_{\text{DS}}$ ,  $\Delta I/I_0$  over five devices at increasing NAG<sub>3</sub> concentrations with respect to the initial current value  $I_0$  (i.e. when no NAG<sub>3</sub> is present in solution).<sup>[58]</sup> We calculated the curves at different  $V_{\text{GS}}$  values: the results extracted for  $V_{\text{GS}} = -0.3 \text{ V}$  are reported in Figure 4b, where a sigmoidal trend is evident from the best fit curve.

It is also apparent that the transconductance increases and that the transfer curves shift towards more positive values of the threshold voltage, thus mirroring the trend of the relative current variation. These trends are reported in Figure 4c and 4d, respectively. The multiparametric variation upon exposure to NAG<sub>3</sub> hints to the fact that the interaction between NAG<sub>3</sub> and the enzyme may act both on the Fermi level of the (6,5)CNTs and on the carrier mobility and/or total charge density of the LZ/(6,5)CNT hybrid after interaction with NAG. The subsequent reorganization of the hydration shells and ion distribution in the proximity of the (6,5)CNT bundles would lead to a more effective gating potential, especially when the sensor is operated in the subthreshold regime.<sup>[59]</sup>

To understand why the device responds so effectively to the presence of NAG<sub>3</sub>, we fitted the dose curves with Langmuir model:

$$\left(\frac{\Delta I}{I_0}\right) = \left(\frac{\Delta I}{I_0}\right)_{\text{max}} \cdot \frac{K_a [\text{NAG}_3]}{1 + K_a [\text{NAG}_3]}$$

(1)

to extract  $K_a$  that is the association equilibrium constant of the LZ-NAG<sub>3</sub> pair at the semiconductor/electrolyte interface.

The  $K_a$  extracted by fitting the curve in Figure 4b, which was obtained in the subthreshold regime, with the Langmuir model is  $(2.1 \pm 0.1) \cdot 10^5 \text{ M}^{-1}$ . As discussed in previous works,<sup>[60–64]</sup> we notice that the transistor sensitivity (derivative of the device response with respect to [NAG<sub>3</sub>] and  $K_a$ ) depend on the applied  $V_{GS}$  (**Figure S7**), although no dramatic changes are observed in the potential window that we investigated (ranging from -0.3 V to -0.5 V), see **Table S2**.

Interestingly, the values of  $K_a$  obtained with our LZ/(6,5)CNT transistor biosensor are comparable to the reported values for lysozyme/NAG<sub>3</sub> interaction in solution. In **Table S3** we report the values measured by different technique and expressed as  $K_d = 1/K_a$ . The  $K_d$  value that we obtain at  $V_{GS} = -0.3$  is  $(4.8 \pm 0.3) \mu\text{M}$ , in line with published values that are invariably in the  $\mu\text{M}$  range, although they were obtained with lysozyme and NAG<sub>3</sub> freely diffusing in solution.

### 3. Conclusion

To conclude, the dispersion of a selected CNT by the lysozyme protein was carried out in water. At odds with other dispersants such as the SDS surfactant, the protein disperses the (6,5)CNT monomolecularly while preserving the electronic properties of the tubes. The solution was drop cast on a silicon substrate where Au source and drain electrodes are interdigitated. The device was first tested as a transistor with the transfer curves of many devices that shows remarkably high reproducibility, which is due to the presence of a single type of CNT. Working devices could be obtained even reducing the LZ/(6,5)CNT concentration from 150  $\mu\text{g/ml}$  to 1.5  $\mu\text{g/ml}$ , observing only a moderate worsening of the electrical performances. In particular, the use of a diluted solution yields an increase in the leakage current that we ascribe to higher exposure of the

interdigitated S and D electrodes to the electrolyte rather than changes in the semiconducting film morphology. Biorecognition is then demonstrated using increasing concentrations of N-acetyl glucosamine trisaccharide (NAG<sub>3</sub>), is a well-known substrate analogue/inhibitor of lysozyme and found to be highly sensitive. Analysis of the device output signal shows that the binding constant of aqueous lysozyme NAG<sub>3</sub> is retained. The present approach is general and can be used to fabricate a new class of highly stable, robust biosensors in a green way.

## ASSOCIATED CONTENT

### **Supporting Information.**

Details on materials and methods; UV-vis absorption spectra and AFM images of Lysozyme and SDS dispersion of (6,5)CNT; electrical characterization of LZ/(6,5)CNT and SDS/(6,5)CNT transistors on silicon and quartz; K<sub>d</sub> values for LZ/NAG<sub>3</sub> couple from literature.

## AUTHOR INFORMATION

### **Corresponding Author**

\* [carloaugusto.bortolotti@unimore.it](mailto:carloaugusto.bortolotti@unimore.it)

\* [matteo.calvaresi3@unibo.it](mailto:matteo.calvaresi3@unibo.it)

### **Author Contributions**

The manuscript was written through contributions of all authors. All authors have given approval to the final version of the manuscript.



## **Funding Sources**

FV was partly supported by the Horizon 2020 Framework Programme under the grant FETOPEN-801367 evFOUNDRY. MDG was supported by a FIRC-AIRC fellowship for Italy (id. 22318). The authors thank PRIN2017-NiFTy (2017MYBTXC) for support.

## REFERENCES:

- [1] J. Wang, *Chem. Rev.* **2007**, *108*, 814.
- [2] M. L. Kringelbach, N. Jenkinson, S. L. F. Owen, T. Z. Aziz, *Nat. Rev. Neurosci.* **2007**, *8*, 623.
- [3] U. Slawinska, S. Rossignol, D. J. Bennett, B. J. Schmidt, A. Frigon, K. Fouad, L. M. Jordan, *Science (80-. )*. **2012**, *338*, 328.
- [4] D. Gao, K. Parida, P. S. Lee, *Adv. Funct. Mater.* **2020**, *30*, 1907184.
- [5] A. Zhang, C. M. Lieber, *Chem. Rev.* **2016**, *116*, 215.
- [6] X. Duan, C. M. Lieber, *Nano Res.* **2015**, *8*, 1.
- [7] Z. Yao, C. L. Kane, C. Dekker, *Phys. Rev. Lett.* **2000**, *84*, 2941.
- [8] A. Javey, H. Kim, M. Brink, Q. Wang, A. Ural, J. Guo, P. McIntyre, P. McEuen, M. Lundstrom, H. Dai, *Nat. Mater.* **2002**, *1*, 241.
- [9] T. Dürkop, S. A. Getty, E. Cobas, M. S. Fuhrer, *Nano Lett.* **2004**, *4*, 35.
- [10] S. Rosenblatt, Y. Yaish, J. Park, J. Gore, V. Sazonova, P. L. McEuen, *Nano Lett.* **2002**, *2*, 869.
- [11] V. Derenskyi, W. Gomulya, J. M. S. Rios, M. Fritsch, N. Fröhlich, S. Jung, S. Allard, S. Z. Bisri, P. Gordiichuk, A. Herrmann, U. Scherf, M. A. Loi, *Adv. Mater.* **2014**, *26*, 5969.
- [12] G. Hills, C. Lau, A. Wright, S. Fuller, M. D. Bishop, T. Srimani, P. Kanhaiya, R. Ho, A.

- Amer, Y. Stein, D. Murphy, Arvind, A. Chandrakasan, M. M. Shulaker, *Nature* **2019**, 572, 595.
- [13] H. Shimotani, S. Tsuda, H. Yuan, Y. Yomogida, R. Moriya, *Adv. Funct. Mater.* **2014**, 24, 3305.
- [14] N. Wei, P. Laiho, A. T. Khan, A. Hussain, A. Lyuleeva, S. Ahmed, Q. Zhang, Y. Liao, Y. Tian, E. Ding, Y. Ohno, E. I. Kauppinen, *Adv. Funct. Mater.* **2020**, 30, 1907150.
- [15] G. S. Tulevski, A. L. Falk, *Adv. Funct. Mater.* **2020**, 30, 1909448.
- [16] C. Zhao, D. Zhong, J. Han, L. Liu, Z. Zhang, L. Peng, *Adv. Funct. Mater.* **2019**, 29, 1808574.
- [17] B. L. Allen, P. D. Kichambare, A. Star, *Adv. Mater.* **2007**, 19, 1439.
- [18] W. S. Wong, A. Salleo, *Flexible Electronics: Materials and Applications*, **2009**.
- [19] V. Schroeder, S. Savagatrup, M. He, S. Lin, T. M. Swager, *Chem. Rev.* **2019**, 119, 599.
- [20] H.-E. Jin, C. Zueger, W.-J. Chung, W. Wong, B. Y. Lee, S.-W. Lee, *Nano Lett.* **2015**, 15, 7697.
- [21] X. Xu, P. Clément, J. Eklöf-Österberg, N. Kelley-Loughnane, K. Moth-Poulsen, J. L. Chávez, M. Palma, *Nano Lett.* **2018**, 18, 4130.
- [22] A. Star, J.-C. P. Gabriel, K. Bradley, G. Grüner, *Nano Lett.* **2003**, 3, 459.
- [23] K. Bradley, M. Briman, A. Star, G. Grüner, *Nano Lett.* **2004**, 4, 253.

- [24] H. S. Song, O. S. Kwon, S. H. Lee, S. J. Park, U.-K. Kim, J. Jang, T. H. Park, *Nano Lett.* **2013**, *13*, 172.
- [25] T. Murugathas, H. Y. Zheng, D. Colbert, A. V. Kralicek, C. Carraher, N. O. V. Plank, *ACS Appl. Mater. Interfaces* **2019**, *11*, 9530.
- [26] Y. Liang, M. Xiao, D. Wu, Y. Lin, L. Liu, J. He, G. Zhang, L.-M. Peng, Z. Zhang, *ACS Nano* **2020**, *14*, 8866.
- [27] D. Tasis, N. Tagmatarchis, A. Bianco, M. Prato, *Chem. Rev.* **2006**, *106*, 1105.
- [28] F. Scuratti, J. M. Salazar-Rios, A. Luzio, S. Kowalski, S. Allard, S. Jung, U. Scherf, M. A. Loi, M. Caironi, *Adv. Funct. Mater.* **2020**, 2006895.
- [29] R. J. Chen, S. Bangsaruntip, K. A. Drouvalakis, N. Wong Shi Kam, M. Shim, Y. Li, W. Kim, P. J. Utz, H. Dai, *Proc. Natl. Acad. Sci.* **2003**, *100*, 4984.
- [30] A. Antonucci, J. Kupis-Rozmysłowicz, A. A. Boghossian, *ACS Appl. Mater. Interfaces* **2017**, *9*, 11321.
- [31] M. Calvaresi, F. Zerbetto, *Acc. Chem. Res.* **2013**, *46*, 2454.
- [32] J. López-Andarias, S. H. Mejías, T. Sakurai, W. Matsuda, S. Seki, F. Feixas, S. Osuna, C. Atienza, N. Martín, A. L. Cortajarena, *Adv. Funct. Mater.* **2018**, *28*, 1704031.
- [33] N. K. Mehra, V. Mishra, N. K. Jain, *Biomaterials* **2014**, *35*, 1267.
- [34] Y. Choi, T. J. Olsen, P. C. Sims, I. S. Moody, B. L. Corso, M. N. Dang, G. A. Weiss, P. G. Collins, *Nano Lett.* **2013**, *13*, 625.

- [35] Y. Choi, I. S. Moody, P. C. Sims, S. R. Hunt, B. L. Corso, I. Perez, G. A. Weiss, P. G. Collins, *Science* (80-. ). **2012**, 335.
- [36] S. Marchesan, M. Prato, *Chem. Commun.* **2015**, 51, 4347.
- [37] M. Di Giosia, F. Valle, A. Cantelli, A. Bottoni, F. Zerbetto, E. Fasoli, M. Calvaresi, *Carbon N. Y.* **2019**, 147, 70.
- [38] H. J. Salavagione, A. M. Díez-Pascual, E. Lázaro, S. Vera, M. A. Gómez-Fatou, *J. Mater. Chem. A* **2014**, 2, 14289.
- [39] A. S. R. Bati, L. Yu, M. Batmunkh, J. G. Shapter, *Adv. Funct. Mater.* **2019**, 29, 1902273.
- [40] M. Chen, X. Fu, Z. Chen, J. Liu, W. Zhong, *Adv. Funct. Mater.* **2020**, 2006744.
- [41] M. Calvaresi, S. Hoefinger, F. Zerbetto, *Chem. - A Eur. J.* **2012**, 18, 4308.
- [42] R. Contreras-Montoya, G. Escolano, S. Roy, M. T. Lopez-Lopez, J. M. Delgado-López, J. M. Cuerva, J. J. Díaz-Mochón, N. Ashkenasy, J. A. Gavira, L. Álvarez de Cienfuegos, *Adv. Funct. Mater.* **2018**, 29, 1807351.
- [43] A. M. Münzer, W. Seo, G. J. Morgan, Z. P. Michael, Y. Zhao, K. Melzer, G. Scarpa, A. Star, *J. Phys. Chem. C* **2014**, 118, 17193.
- [44] M. S. Filipiak, M. Rother, N. M. Andoy, A. C. Knudsen, S. Grimm, C. Bachran, L. K. Swee, J. Zaumseil, A. Tarasov, *Sensors Actuators, B Chem.* **2018**, 255, 1507.
- [45] K. Maehashi, T. Katsura, K. Kerman, Y. Takamura, K. Matsumoto, E. Tamiya, *Anal. Chem.* **2007**, 79, 782.

- [46] H. Gong, F. Chen, Z. Huang, Y. Gu, Q. Zhang, Y. Chen, Y. Zhang, J. Zhuang, Y.-K. Cho, R. H. Fang, W. Gao, S. Xu, L. Zhang, *ACS Nano* **2019**, *13*, 3714.
- [47] D. Nepal, K. E. Geckeler, *Small* **2006**, *2*, 406.
- [48] H. Nie, H. Wang, A. Cao, Z. Shi, S.-T. Yang, Y. Yuan, Y. Liu, *Nanoscale* **2011**, *3*, 970.
- [49] S. Reich, C. Thomsen, P. Ordejón, *Phys. Rev. B* **2002**, *65*, 155411.
- [50] F. Scuratti, G. E. Bonacchini, C. Bossio, J. M. Salazar-Rios, W. Talsma, M. A. Loi, M. R. Antognazza, M. Caironi, *ACS Appl. Mater. Interfaces* **2019**, *11*, 37966.
- [51] L. Hu, D. S. Hecht, G. Grüner, *Nano Lett.* **2004**, *4*, 2513.
- [52] J. Rivnay, P. Leleux, M. Ferro, M. Sessolo, A. Williamson, D. a. Koutsouras, D. Khodagholy, M. Ramuz, X. Strakosas, R. M. Owens, C. Benar, J.-M. Badier, C. Bernard, G. G. Malliaras, *Sci. Adv.* **2015**, *1*, e1400251.
- [53] C. M. Proctor, J. Rivnay, G. G. Malliaras, *J. Polym. Sci. Part B Polym. Phys.* **2016**, *54*, 1433.
- [54] D. Nepal, S. Balasubramanian, A. L. Simonian, V. A. Davis, *Nano Lett.* **2008**, DOI 10.1021/nl080522t.
- [55] D. W. Horn, K. Tracy, C. J. Easley, V. A. Davis, *J. Phys. Chem. C* **2012**, *116*, 10341.
- [56] M. M. Noor, J. Goswami, V. A. Davis, *ACS Omega* **2020**, *5*, 2254.
- [57] J. C. Cheetham, P. J. Artymiuk, D. C. Phillips, *J. Mol. Biol.* **1992**, *224*, 613.

- [58] F. N. Ishikawa, M. Curreli, H.-K. Chang, P.-C. Chen, R. Zhang, R. J. Cote, M. E. Thompson, C. Zhou, *ACS Nano* **2009**, 3, 3969.
- [59] X. P. A. Gao, G. Zheng, C. M. Lieber, *Nano Lett.* **2010**, 10, 547.
- [60] M. Berto, S. Casalini, M. Di Lauro, S. L. Marasso, M. Cocuzza, D. Perrone, M. Pinti, A. Cossarizza, C. F. Pirri, D. T. Simon, M. Berggren, F. Zerbetto, C. A. Bortolotti, F. Biscarini, *Anal. Chem.* **2016**, 88, 12330.
- [61] C. Diacci, M. Berto, M. Di Lauro, E. Bianchini, M. Pinti, D. T. Simon, F. Biscarini, C. A. Bortolotti, *Biointerphases* **2017**, 12, 05F401.
- [62] M. Berto, C. Diacci, R. D'Agata, M. Pinti, E. Bianchini, M. Di Lauro, S. Casalini, A. Cossarizza, M. Berggren, D. Simon, G. Spoto, F. Biscarini, C. A. Bortolotti, M. Di Lauro, S. Casalini, A. Cossarizza, M. Berggren, D. Simon, G. Spoto, F. Biscarini, C. A. Bortolotti, *Adv. Biosyst.* **2018**, 2, 1700072.
- [63] M. Berto, E. Vecchi, L. Baiamonte, C. Condò, M. Sensi, M. Di Lauro, M. Sola, A. De Stradis, F. Biscarini, A. Minafra, C. A. Bortolotti, *Sensors Actuators, B Chem.* **2019**, 281.
- [64] M. Sensi, M. Berto, S. Gentile, M. Pinti, A. Conti, G. Pellacani, C. Salvarani, A. Cossarizza, C. A. Bortolotti, F. Biscarini, *Chem. Commun.* **2021**, 57, 367.